33

74037

ICRL-70524

AMPTIAC

A Facsimile Report

Reproduced by
UNITED STATES
ATOMIC ENERGY COMMISSION
Division of Technical Information
P.O. Box 62 Oak Ridge, Tennessee 37830

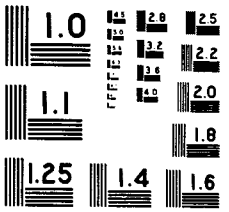

UCRL - 70524
PREPRINT

Conf-680603--2

Lawrence Radiation Laboratory
UNIVERSITY OF CALIFORNIA
LIVERMORE

ELEVATED TEMPERATURE DEFORMATION AND ELECTRON MICROSCOPE STUDIES OF POLYCRYSTALLINE TUNGSTEN AND TUNGSTEN-RHENIUM ALLOYS

Richard R. Vandervoort
Willis L. Barmore

October 1, 1968

This paper was prepared for publication in the Proceedings of the Sixth Plansee Seminar, Reutte-Tyrol, Austria, June 24-28, 1968.

44

Elevated Temperature Deformation and Electron Microscope Studies of Polycrystalline Tungsten and Tungsten-Rhenium Alloys

Richard R. Vandervoort and Willis L. Barmore
Lawrence Radiation Laboratory, University of California
Livermore, California

ABSTRACT

Tungsten, tungsten-25 wt. % rhenium and tungsten-30 wt. % rhenium were plastically deformed from 1400 to 1900°C at stresses up to 10,000 psi in a vacuum of less than 10^{-8} torr. The activation energy for creep and the relationship between stress and strain rate were determined. Effects of thermo-mechanical history, composition, and grain size on strain rate were also investigated. Dislocation substructure was studied by etch pit and transmission electron microscope techniques, and these observations were correlated with the creep data. The factors important in the high-temperature deformation of these materials were analyzed, and the experimental results were rationalized in terms of current theories for rate-controlling deformation mechanisms.

INTRODUCTION

The creep behavior of materials at elevated temperatures is dependent on factors such as diffusivity,[1] stress, elastic moduli,[2] stacking fault energy,[3] and grain size.[4-7] Analysis of creep data for many polycrystalline

This work was performed under the auspices of the U. S. Atomic Energy Commission.

metals and alloys at high temperatures shows that the deformation rate can be described by the following relation:[4,8]

$$\dot{\epsilon} = C\, f(s) \left(\frac{\sigma}{E}\right)^n D \qquad [1]$$

where

$\dot{\epsilon}$ = minimum creep rate

C = constant

f(s) = a function involving microstructure

σ = applied stress

E = the average elastic modulus at test temperature

n = constant

D = diffusion coefficient.

In general, a material with higher elastic modulus and lower diffusion coefficient should have greater creep resistance at constant stress, constant temperature, and equivalent microstructures. At temperatures greater than 1100°C, few metals and alloys retain appreciable strength. Likely materials for structural use above this temperature are metals or alloys of the group VB and VIB elements.

The data from dynamic measurements of elastic moduli with temperature for polycrystalline tungsten, molybdenum, tantalum, and niobium are shown in Fig. 1.[9,10] Tungsten apparently has the advantage at all temperatures. Diffusion coefficients for these metals are shown in Fig. 2. Various investigations on diffusion in niobium,[11-13] molybdenum,[14-16] and tantalum[17,18] are in good agreement, whereas significant differences exist between the two sets of data for tungsten.[19,20] In both cases, however, extrapolated diffusion coefficients for tungsten are lower than those for the other metals.

On the basis of Eq. [1] and the data in Figs. 1 and 2, tungsten and its alloys should have superior creep resistance at high temperatures when compared to other materials. In this work the creep behavior of tungsten, W-25 Re, and W-30 Re were studied.*

*W-25 Re and W-30 Re refer to tungsten 25 and 30 wt. % Re respectively.

The creep of pure tungsten has been studied by several investigators,[21-27] but little information has been reported on the correlation of creep properties with microstructure. One of the primary goals of this investigation was to evaluate the relationship between creep behavior and microstructure for tungsten as well as W-25 Re and W-30 Re. In addition, the creep behavior of tungsten was studied to provide reference data for comparison with creep data for W-25 Re and W-30 Re.

The compositions W-25 Re and W-30 Re were selected for study because the former is a solid solution alloy, and the latter a two-phase alloy up to 2000°C (Fig. 3).[28] Thus, the properties of the two types of tungsten alloys could be compared.

In this investigation tungsten, W-25 Re and W-30 Re were creep-tested in tension from 1400° to 1900°C at stresses from 1500 to 10,000 psi. The effect of temperature, stress, composition, and grain size on creep rate were determined. Transmission electron microscope and etch pit techniques were used to study dislocation substructure developed during high-temperature deformation, and the results were correlated with creep data.

MATERIALS AND EXPERIMENTAL TECHNIQUES

All materials used in this study were consolidated using high-purity powders. After compaction, the following fabrication schedules were used:

Tungsten:

1. Sintered in hydrogen at 2600°C for 4 hr.
2. Extruded to sheet bar 0.250 in. at 1800°C.
3. Reduced to 0.100 in. by rolling at 1400°C.
4. Recrystallized at 1300°C for 1 hr.
5. Reduced to 0.050 in. by rolling at 1400-1100°C.
6. Stress-relieved at 1100°C for 1 hr.

W-25 Re:

1. Sintered in hydrogen at 2400°C for 15 hr.
2. Forged to plate 0.250 in. at 1800°C.
3. Reduced to 0.090 in. by rolling at 1450°C.
4. Reduced to 0.050 in. by rolling at 1200°C.
5. Stress-relieved at 1300°C for 1 hr.

W-30 Re:

1. Sintered in hydrogen at 2400°C for 15 hr.
2. Dynapak extruded to sheet bar 0.400 in. at 2000°C.
3. Reduced to 0.180 in. by rolling at 1600°C.
4. Recrystallized at 2100°C for 1/2 hr.
5. Reduced to 0.100 in. by rolling at 1450°C.
6. Stress relieved at 1450°C for 1 hr.
7. Reduced to 0.050 in. by rolling at 1450°C.
8. Stress-relieved at 1400°C for 1 hr.

Impurities as determined by general spectrochemical analyses of the as-received materials are listed in Table I. Hydrogen, carbon, nitrogen and oxygen contents are also shown. No significant changes in impurity content were found in creep-tested specimens exposed for as long as 500 hr at pressures of about 10^{-8} torr and temperatures greater than 1400°C.

Creep specimens were cored to approximate shape from the as-received plates by spark discharge machining, and finished ground to final dimensions by conventional methods.

Test specimens were 2.5 in. in overall length and 0.050 in. thick, and had a gage length of 0.75 in. and gage width of 0.125 in. Fiducial marks for strain measurement were drilled into the specimen by a spark discharge process using a 0.010-in. tungsten wire.

To produce a stable grain size before creep testing, tungsten and W-25 Re specimens were annealed at 1800°C for 50 hr and W-30 Re specimens were solution-treated at 2250°C for 2 hr and aged at 1800°C for 50 hr. After these thermal treatments the grain sizes of the tungsten, W-25 Re and W-30 Re were 34 ± 4, 27 ± 4, and 104 ± 8 microns respectively, as determined by the intercept method.

Before metallographic examination, the tungsten was etched in a solution of 5 g NaOH and 30 g $K_3Fe(CN)_6$ in 100 ml of distilled water. The two W-Re alloys were etched in a solution of two parts 25 wt. pct solution of $CuSO_4$ and one part NH_4OH.

All creep tests and annealing treatments were conducted in a vacuum of less than 10^{-8} torr. The stainless steel vacuum chamber was sealed at joints with high-purity copper gaskets. VacSorb pumps were used to obtain an initial pressure of 10^{-2} torr, and then a 500 liter/sec ion pump and accessory titanium sublimation filaments were employed to achieve pressures

of less than 10^{-8} torr. The test furnace consisted of a tungsten mesh heating element 2 in. in diameter and 7 in. in length, tungsten heat shields, and a water-cooled copper shell. The maximum temperature capability was 2400°C.

The basic components of the temperature control system were a thermal-watt converter, recorder-controller, and silicon control rectifier unit. Temperature was measured by an optical pyrometer which had been calibrated with a standard filament. The temperatures reported were obtained by adding a correction factor for the sight port glass to the optical pyrometer reading. There were no detectable temperature gradients along the test specimen.

Tensile loads were applied to specimens through a bellows arrangement. Tungsten force rods 1 in. in diameter were used in the hot section of the load column. Stresses were maintained to ±1% of the selected value by periodic weight corrections to compensate for changes in specimen cross-sectional area during deformation and for changes in the bellows spring force due to load column extension.

Deformation at temperature was determined by measuring the distance between fiducial marks on the gage section of the specimen with an optical comparator. Total deformation was also obtained by measuring the gage length before and after testing at room temperature. Total deformation measured at high temperature and room temperature agreed within 2%.

Specimens for substructure studies were cut from the gage section, and then were planed to a thickness of around 0.010 in. by spark discharge machining. These pieces were thinned for viewing in the electron microscope by electropolishing. The window technique was employed for

this purpose. The conditions and solutions used for electropolishing the materials are listed in Table II. The foils were examined in a Siemens Elmiskop I operating at a potential of 100 kV.

Etch pit methods were used to study dislocation substructure in creep-tested tungsten specimens. After conventional polishing, the surface was electropolished at 15 volts in a 2% NaOH solution to remove surface damage, and then etch pitted for about 2 sec in the same solution at a potential of 3 volts.

Large grain size creep specimens of tungsten and W-25 Re were obtained by annealing at 2400°C for 5 hr. This heat treatment produced grain sizes of 125 and 450 microns respectively. These specimens were used in the determination of grain size effect on creep rate.

EXPERIMENTAL RESULTS

Plastic deformation of polycrystalline solids under moderate stresses and at temperatures above one-half the melting point (absolute units) usually involves thermally activated processes. Under these conditions the minimum creep rate of many metals and alloys is given by the following equation:

$$\dot{\epsilon} = K f(s) \sigma^n e^{-\Delta H/RT} \qquad [2]$$

where

K = constant

ΔH = apparent activation energy for creep

R = gas constant

T = absolute temperature.

This relation is implicit in Eq. [1], but is more useful in analyzing creep data. From this expression the stress, temperature, and microstructure effects on strain rate can be evaluated.

The stress exponent n was determined by using the incremental change in stress technique. In this method temperature was held constant, and strain rates from a single specimen were measured at several different stresses. The apparent activation energy for creep ΔH was determined by using the incremental change in temperature technique. In this case, stress was held constant and strain rates from a single specimen were measured at various temperatures. The relationship between f(s) and creep behavior was found by correlating observations on the microstructure of plastically deformed specimens with creep data from constant stress-constant temperature tests.

Creep Curves. Standard-type creep curves, where stress and temperature are held constant, were obtained for tungsten, W-25 Re, and W-30 Re. These tests were used to determine the extent of primary and secondary creep strain. This information is important since the total strain at any time, as well as the rate at which strain accumulates, are both design criteria.

Standard creep curves, typical for each of the materials, are shown in Fig. 4. Tungsten has a significant amount of primary creep, whereas the W-25 Re and W-30 Re had negligible primary creep. Thus, in high-temperature structural uses of tungsten where small total deformation is required, prestraining tungsten into the region of secondary creep could prove advantageous in maintaining dimensional stability. The creep curves for all the materials also had extensive regions of secondary creep, and

thus Eq. [2] could be used to evaluate the effect of stress and temperature on the minimum creep rate. In a few instances creep curves exhibited tertiary creep at strains greater than 5 %; however, data involving tertiary creep were not included in the analyses.

Stress Effect on Creep Rate. The types of strain-time curves obtained from change of stress tests are illustrated in Fig. 5. Tungsten exhibited an appreciable amount of primary creep at each stress, as was the case for the standard creep tests. On the other hand, the strain-time curves for W-25 Re and W-30 Re, exhibited no dectable primary creep after initial loading or after subsequent changes of stress.

The dependence of strain rate on the applied tensile stress at various temperatures for tungsten, W-25 Re, and W-30 Re, are shown in Figs. 6-8. A particular curve represents data obtained from a single specimen at constant temperature. After a minimum creep rate was measured at a given stress, the stress was abruptly changed to a new level. The average stress exponent n for tungsten was 5.8, indicating a relatively high creep-rate sensitivity to stress (Fig. 6). The average stress exponent for the W-25 Re alloy was 3.8 over the stress range 5,000-10,000 psi (Fig. 7). However, the stress effect on strain rate below 5000 psi is apparently less than that at higher stresses. In order to verify the change in slope on the stress-strain rate curves for W-25 Re, another specimen was tested at 1500 psi at 1500-1800°C, and these data points are designated by solid symbols on the graph. These results are further evidence of the existence of inflections in the stress-strain rate curves for W-25 Re. The average stress exponent for the W-30 Re alloy was also 3.8 (Fig. 8).

Temperature Effect on Creep Rate. Characteristic strain-time curves from change of temperature tests are illustrated in Fig. 9. After initial

loading the tungsten again showed a region of primary creep, but no further transients were seen after changes to subsequent temperatures. No primary creep was observed during change of temperature tests for W-25 Re and W-30 Re.

The influence of temperature on strain rate at different stresses for the materials studied appears in Figs. 10-12. The apparent activation energy for creep of tungsten (Fig. 10) and W-30 Re (Fig. 12) was approximately 100 kcal/mole, and was insensitive to the applied stress. At stresses of 5000 psi and above, the activation energy for W-25 Re was also about 100 kcal/mole (Fig. 11). However, the activation energy for creep decreases with decreasing stress below 3500 psi. These results are consistent with the inflections in the stress-strain rate curves for W-25 Re (Fig. 7).

Grain Size Effects. As a result of the pretest thermal treatments, specimens of a given type had similar grain sizes. These annealing treatments were used to minimize specimen-to-specimen variation in creep properties. The grains were equiaxed, and the grain size was approximately the same in both the transverse and longitudinal directions. Specimens of tungsten and W-25 Re sectioned from as-received plates parallel to and perpendicular to the primary rolling direction had essentially the same creep rate for a given stress and temperature.

In some cases, the creep of metals and alloys at elevated temperature is reportedly influenced by grain size.[4-7] Standard creep tests and change of stress tests were run on large-grained tungsten and W-25 Re at 1700°C. No appreciable differences were found in creep rates or stress exponents for tungsten where the large and small grain sizes were 125 and 34 microns, respectively. Creep data for tungsten, shown in Figs. 6 and 10, are from

small grain size specimens. Creep data for W-25 Re at two different grain sizes are shown in Fig. 13. At high stresses, the strain rates and stress exponents for coarse- and fine-grained material were in good agreement. For the large-grained specimen (450 μ), the strain rate was proportional to stress to the 3.8 power over the entire range of stress investigated; whereas, the stress-strain rate relation for the small-grained material (27 μ) deviated from the power law below 5000 psi. The stress exponent in the low stress region was about one.

The stress effect on creep rate for W-25 Re was dependent on grain size at low stresses (Fig. 7), and as a consequence the activation energy for creep of coarse- and fine-grained material was determined at a stress of 2500 psi. The activation energy for the large-grained specimen was 105 kcal/mole and that for the small-grained specimen was 63 kcal/mole. The ΔH value of 105 kcal/mole was in close agreement with the values for fine-grained W-25 Re at high stresses.

Dislocation Substructure. Creep properties of crystalline materials are generally sensitive to substructure. Substructure could be a function of stress, temperature, or strain. Standard creep tests were run at various conditions to establish the effect of stress and temperature on dislocation density and subgrain size. The specimens were creep-tested to 5 pct strain, and then cooled to room temperature under load to prevent dislocation rearrangement. In all cases, a strain of 5% was well into the steady-state region of creep, and the dislocation substructure was in dynamic equilibrium. It has been demonstrated that in the region of secondary creep, dislocation density and sub-grain size are independent of strain.[29,30]

Thin foils from the gage section of creep-tested specimens were examined in the electron microscope. The arrangement and distribution of dislocations for tungsten and those for the W-Re alloys were distinctly different. In creep-tested tungsten, a well-defined subgrain structure was observed as well as individual dislocations within the subgrains. The cell walls consisted of regular networks or dense tangles of dislocations. Representative examples of networks in creep-tested tungsten are shown in Fig. 14. On the other hand, essentially no subgrain formation was observed and networks were seen infrequently in W-25 Re and W-30 Re. In addition, the dislocation density in the networks found in W-Re alloys was lower than that found in the nets in tungsten. Often the dislocation in the two alloys were arranged in simple tilt boundaries. Dislocation arrays in creep-tested W-25 Re and W-30 Re are illustrated in Figs. 15 and 16.

Crystallographic analyses of the dislocation configurations in Figs. 14a, 14b, and 16a show that the networks are not comprised of pure edge dislocations but could be comprised of pure screw dislocations. Analyses of the dislocations in Figs. 15a, 15b, and 16b indicate that the dislocations are principally either in pure edge or pure screw orientation. However, contrast experiments to determine Burgers vectors were unsuccessful because of the combination of high bulk densities and foil thicknesses.

Subgrain size in deformed tungsten was obtained from electron micrographs by averaging the longest and shortest cell dimensions in at least 40 subgrains in each sample. Subgrain size was also determined by the etch pit technique in an analogous manner. The results from both methods agreed within a factor of one and one-half (Fig. 17). In each

case, the subgrain size was inversely proportional to the applied stress. Data on subgrain size as a function of stress for other materials are also shown.[31-33] These results suggest the relation $\lambda \sim 1/\sigma$ may be generally applicable to the creep behavior of many materials. Subgrain sizes in specimens creep tested at 1500 and 1800°C at a stress of 5000 psi were essentially the same size as the subgrain size found at 1700°C and 5000 psi. Typical micrographs of subgrains in tungsten deformed at high temperature are given in Fig. 18. No subgrains were found in pretest specimens.

Dislocation density was determined from the relation:

$$\rho = \frac{k\,N}{A} \qquad [3]$$

where

ρ = length of dislocation line per unit volume

k = proportionality constant for conversion from area dislocation density to volume dislocation density ($k \approx 2$)[34]

N = total number of dislocation intersections with both foil surfaces

A = total area of both foil surfaces.

The area method of counting[35] had the advantages that localized rotation of dislocations did not affect the results, and foil thicknesses were not required. In the density determinations, only dislocations not associated with subboundaries or networks were counted. Several foils from each specimen were examined, and the dislocation densities reported were obtained from the average of a minimum of 10 areas. To avoid edge effects, only areas away from the edge of the foil were sampled.

Dislocation densities for tungsten, W-25 Re and W-30 Re as determined by electron microscopy, can be described by the following expression,

$\rho \sim \sigma^{2.3}$ (Fig. 19). These results have been corrected for dislocations in specific crystallographic orientations which are invisible because of unfavorable contrast conditions.[36] Typical electron micrographs of dislocation density corresponding to particular stresses for W-25 Re are illustrated in Fig. 20.

The dislocation density in creep-tested tungsten was also determined by etch pitting (Fig. 19). Etch pit measurements were made on the same tungsten specimens later used for dislocation density determinations by transmission electron microscopy. Results from the two techniques were in good agreement at lower stresses, but diverged at high stresses. The sodium hydroxide etch gave reproducible etch pit patterns, but the difference in dislocation densities from the two methods could result because some dislocations intersecting the surface do not etch and/or some etch pits represent more than one dislocation. These effects would cause a low bias in the etch pit densities and would be more pronounced at higher dislocation densities. Other studies also indicate etch pit results were lower than those determined by electron microscopy.[37,38]

DISCUSSION

Tungsten. The deformation of tungsten at elevated temperatures has been investigated at a wide variety of strain rates and temperatures. Early work on tungsten was done at relatively low[26] and relatively high[24] temperatures. More recent efforts have been concentrated in the intermediate temperature region of 1400-2100°C,[21-23,25,27] and this is the range where tungsten will probably have its greatest potential application.

In the present work, the strain rate of tungsten at 1400-1800°C was proportional to stress to the 5.8 power (Fig. 6). This power stress law was

valid between 2500 and 10,000 psi, and the stress exponent was independent of temperature in the region studied. Other investigators have reported a similar high sensitivity of strain rate to stress for tungsten at intermediate temperatures. The stress exponent appearing in Eqs. [1] and [2] is usually in the range 4-5 for most pure metals.[4,8] However, large values of n at high strain rates are not uncommon in other metals, and this higher strain-rate sensitivity to stress results from excess lattice vacancies generated at high stress.[39]

The activation energy for creep of polycrystalline solids above one-half the melting point usually corresponds to an activation energy for diffusion.[40] The activation energy for creep of tungsten above 2200°C has been reported to be 141 and 160 kcal/mole,[21,24,41] and these values are in reasonable agreement with the activation energy for volume self-diffusion in single crystal tungsten of 153 kcal/mole.[19]

The apparent activation energy for creep of polycrystalline tungsten found in the present work was around 100 kcal/mole and was insensitive to the applied stress (Fig. 10). A recent analysis of creep data of polycrystalline tungsten revealed at least two distinct activation energies for creep.[42] Above 0.67 T_m (°K) an average value for ΔH was 140 kcal/mole. Between 0.5 T_m and 0.67 T_m, ΔH was approximately 100 kcal/mole. Evidently, 100 kcal/mole does not correspond to the activation energy for volume self-diffusion. Activation energies of 100 ± 10 kcal/mole have been reported for sintering, grain boundary, subboundary, and dislocation core diffusion in tungsten.[43-46]

Observations on the dislocation substructure developed during creep and the power stress law strongly suggest that the high-temperature deformation of polycrystalline tungsten occurs by a dislocation mechanism.

Therefore, the rate-controlling diffusion process during creep should involve either subboundary or dislocation core diffusion.

In general, creep curves for pure polycrystalline tungsten have similar characteristics, regardless of processing history. Primary creep strain is typically 1-2% before steady-state creep is established[21,22,24] (Fig. 4). In addition, strain-time curves for tungsten during change-in-stress tests show a transient portion following each incremental increase in stress[21] (Fig. 5). However, during change-in-temperature tests a transient region of creep was observed only after initial application of stress but not after subsequent incremental temperature changes (Fig. 9).

The shape of strain-time curves for pure tungsten can be rationalized in terms of changes occurring in dislocation substructure. Prior to testing, tungsten specimens had a dislocation density of about $10^7/cm^2$ and no subgrains. After testing, two significant changes were evident in the dislocation substructure. The dislocation density had increased appreciably, and a well-defined subgrain network had formed. Both dislocation density and subgrain size were strongly dependent on the applied stress (Figs. 17 and 19). Dislocation densities in W-Re alloys were essentially the same as those for tungsten at equivalent stresses, but the creep curves for the alloys had no primary creep region. Therefore, the transient portion of the creep curves for tungsten must be closely associated with formation of an equilibrium subgrain size after application of the stress.

Further evidence confirming the relationship between subgrain formation and primary creep was obtained from a drop-in-stress test. A specimen was deformed at 6000 psi until steady-state creep was obtained, then the stress was abruptly dropped to 3500 psi. The initial rate immediately

after the decrease in stress was an order of magnitude lower than would be expected if deformation occurred only at 3500 psi (Fig. 21). After the drop in stress, 3 hours were required before the secondary creep rate for 3500 psi was established. During this period, the subgrain diameter increased by almost a factor of two to achieve the equilibrium value for 3500 psi, and the transient portion of the curve after the stress decrease was related to the changing subgrain size. Furthermore, there was no transient creep during change-in-temperature tests (Fig. 9), and subgrain size at constant stress was virtually the same for temperatures in the range 1500-1800°C. These results demonstrate that subgrain size formed during creep of tungsten is insensitive to temperature, as has been previously suggested for aluminum.[31,47] These observations on dislocation substructure formed during high-temperature deformation indicate that significant improvement in the creep strength of tungsten might be obtained by stabilizing a very small subgrain size with an inert dispersoid or a stable precipitate.

The extent of primary creep in tungsten is quite small when compared to primary creep in pure f.c.c. metals. Since slip on more than one system facilitates subgrain formation, cross slip occurred readily or several slip systems operated concurrently at early stages during deformation of polycrystalline tungsten at elevated temperatures.

The dislocation density within the subgrains was a strong function of stress, but was apparently independent of temperature. The density ranged from approximately $10^7/cm^2$ for annealed material to almost $10^9/cm^2$ for specimens creep-tested at 10,000 psi (Fig. 19). Similar dislocation densities at equivalent stresses have also been found in a creep-tested Fe-Si alloy[38] and a Fe-Mn-N alloy.[48] Of particular interest are the results for the Fe-Si alloy where similar methods were used to determine dislocation

densities. Not only do the results agree closely, but the etch pit densities for Fe-Si were less than those determined from transmission electron microscopy by about the same factor as in the present investigation. Since the dislocation densities obtained from thin foils are greater than those obtained from etch pitting of bulk specimens, it is evident that few dislocations are lost during thinning.

The dislocation density was proportional to stress to the 2.3 power. Similar relationships between dislocation density and stress have been found for the creep of Fe and some Fe alloys.[38,49] Several theories of work hardening for low-temperature deformation predict that $\rho \sim \tau^2$ where τ is the flow stress, and this relation has been verified experimentally.[50] In this respect, low- and high-temperature deformation are similar. However, dislocation density does not depend on strain during creep in the secondary region. Thus, the creep process during steady-state deformation is a dynamic equilibrium between generation and recovery of dislocation substructure.

The deformation of polycrystalline tungsten in the temperature range 0.5—0.67 T_m has been studied by a number of investigators,[21-23,25,27] and the apparent activation energy for creep in this region is about 100 ± 10 kcal/mole.[42] The results from six investigations on the creep of tungsten at intermediate temperatures are compared in Fig. 22. Creep rates have been compensated for temperature, using an activation energy of 100 kcal/mole.

As noted previously, the data from all these investigations show a high strain-rate sensitivity to the applied stress. The higher stress exponents shown on the graph are associated with the higher compensated strain rates. This is in accord with theory, which predicts enhanced strain

rates resulting from the contribution of non-equilibrium excess vacancies to the rate of diffusion.[39] All the data in Fig. 22 are in good agreement. The creep results were obtained from specimens which had wide variations in chemical, thermal, and mechanical histories. It is significant that the creep behavior of polycrystalline tungsten in this temperature region is not sensitive to process history, grain size, metallic impurity level, and carbon, oxygen, and nitrogen content.

Dislocation mechanisms controlling the rate of creep of polycrystalline tungsten have been the subject of recent discussions.[51,52] At temperatures greater than about 0.67 T_m (2200°C) there is general agreement that deformation in tungsten is governed by dislocation climb.[53] The activation energy for creep of tungsten at high temperature ranges from 140-160 kcal/mole,[21,24,41] and is in reasonable agreement with the activation energy for self-diffusion of 153 kcal/mole.[19] Therefore, the rate-controlling diffusion process appears to be volume diffusion. In the temperature region 0.5 to 0.67 T_m, both the jogged screw model[38] and dislocation climb model[53] have been proposed as the rate-controlling deformation mechanism during creep.[51,52]

In the present work, the apparent activation energy for creep was 100 kcal/mole over the temperature region 1400°-1900° C and is consistent with the activation energy for sub-boundary or dislocation core diffusion. The activation energy for creep was insensitive to the applied stress, and the stress exponent n did not depend on temperature. The relation between strain rate and stress where $\dot{\epsilon} \sim \sigma^{5.8}$ was valid over the stress range 2500-10,000 psi. Thus, on the basis of these results, it is probable that a single dislocation mechanism controls creep at these temperatures and stresses.

On the basis of the experimental results of the present study, three possible rate-controlling deformation mechanisms for the creep of polycrystalline tungsten are: motion of jogged screw dislocations,[38] dislocation glide,[54] and dislocation climb.[53] At a particular temperature, the creep rate for both the jogged screw model and the dislocation glide model is proportional to the product of the mobile dislocation density and the applied stress. As established in this investigation, the dislocation density in tungsten varies as stress to the 2.3 power, and is independent of temperature. Thus, assuming that the number of mobile dislocations is proportional to the measured dislocation density, creep rate should be a function of stress to the 3.3 power for the jogged screw and dislocation glide mechanisms. Also, strain-time curves for deformation by these mechanisms should exhibit negligible primary creep. Furthermore, at high stresses, the jogged screw model requires an exponential stress law and an activation energy dependent on the applied stress. The foregoing requirements are contrary to experimental observations. On the other hand, the dislocation climb mechanism requires a fifth-power strain-rate dependence on stress,[4] and experimentally a 5.8-power strain-rate dependence on stress was found. Dislocation climb assists in formation of regular three-dimensional subgrain networks, and, as discussed previously, a well-defined subgrain structure developed during creep of polycrystalline tungsten. The above considerations are in general accord with the climb model. Therefore, it is concluded that creep of polycrystalline tungsten at intermediate temperatures is governed by dislocation climb.

Tungsten-Rhenium Alloys. The W-Re alloys are technologically important, and while several studies have been conducted on their low-temperature properties, little work has been reported on the creep properties of these alloys. Available data on the creep of W-25 Re are shown in Fig. 23.[55-57] In this comparison, creep rates were compensated for temperature by employing the activation energy for creep determined in the present work. The dashed lines represent curves derived from only three data points. These data agree within a factor of ten with respect to strain rate or within a factor of two with respect to stress, despite the wide variety of impurity contents and fabrication histories.

The stress exponents from tests on powder metallurgy alloy specimens are in reasonable agreement, but it is not clear whether there is any real difference between stress exponents for arc-cast and powder metallurgy materials. However, the creep curves for W-25 Re are similar regardless of processing history. Steady-state strain rates from standard creep tests were established immediately after loading with no evidence of primary creep. Also, as shown in this investigation, no transients were observed during change of stress tests or change of temperature tests (Figs. 5 and 9).

Dislocation densities in W-Re alloys were a strong function of the applied stress (Fig. 19), but no subgrains formed at any stress or temperature investigated. Primary creep in tungsten was attributed to the formation of a stable subgrain size and since there was no transient creep in W-Re alloys, the equilibrium dislocation density in the W-Re alloys apparently is established very quickly after initial application of a stress and after subsequent changes in stress.

In this study the creep properties of W-25 Re (at high stresses or large grain sizes) and W-30 Re were remarkable similar. The creep curves for these alloys had no measurable primary creep region, and this is not surprising since no subgrain structure formed during deformation. Both alloys had essentially the same activation energy for creep (Figs. 11 and 12), stress effect on strain rate (Figs. 7, 8, 13), and dislocation density dependence on stress (Fig. 19). In addition, secondary creep rates were nearly the same for a given stress and temperature.

At the test temperatures, W-25 Re is a solid solution alloy and W-30 Re is a two-phase alloy with σ phase precipitate in a W-Re matrix (Fig. 3). Aging studies were conducted on W-30 Re from 1400 - 2000° C for various times. Room-temperature hardness measurements showed no significant increase in strength for any aging condition. Light and electron microscopy revealed that σ phase precipitated predominantly in the grain boundaries in an almost continuous layer, but small σ phase particles were observed occasionally in the matrix. Interaction between dislocations and σ phase precipitates within the volume of the grain occurred during creep testing (Fig. 24). However, dislocations interacted with matrix precipitates on such a limited scale that no increase in creep resistance of the W-30 Re alloy was apparent when compared with the creep properties of the W-25 Re alloy. The dislocation-precipitate interactions indicate that if nucleation of σ phase in the matrix could be enhanced, the creep resistance of W-30 Re might be substantially increased.

The apparent activation energy for creep of both W-25 Re (at high stresses) and W-30 Re was about 100 kcal/mole and was the same as that for pure tungsten. The volume diffusion coefficient of rhenium in tungsten is essentially the same as the self-diffusion coefficient of tungsten.[19] If

other diffusion processes such as boundary, surface and dislocation core diffusion are also similar for the tungsten and rhenium atoms in W-Re alloys, the activation energy of 100 kcal/mole probably corresponds to sub-boundary or dislocation core diffusion.[45] Since no subgrains were observed in deformed microstructures, the diffusion process governing creep in W-Re alloys should be dislocation core diffusion.

The beneficial alloying effect of rhenium on the low-temperature properties of tungsten has been documented, but the effect of rhenium on the high-temperature deformation behavior of tungsten is not well-known. In this investigation, the deformation behavior of W-25 Re and W-30 Re were studied under test conditions similar to those used for pure tungsten; thus, the creep properties of the alloys could be compared directly with tungsten. Using the activation energy of 100 kcal/mole, secondary creep rates for tungsten and the W-Re alloys were compensated for temperature by the relation $Z = \dot{\epsilon}\, e^{\Delta H/RT}$, and the results were plotted against the creep stress to elastic modulus ratio (Fig. 25). At a stress-to-modulus ratio of 5×10^{-4}, the creep resistance of tungsten and the W-Re alloys is the same. Since the elastic moduli for tungsten and the alloys are about equivalent at a given temperature, the alloys have a slight advantage in creep resistance at higher stresses and tungsten has a small advantage in creep resistance at lower stresses. It should be noted, however, that the comparison of creep data in Fig. 25 is based on secondary creep rates. When the comparison is made on the basis of total strain at a given time, use of tungsten is less favorable with respect to the W-Re alloys because it exhibits 1-2% primary creep strain before entering the secondary region while the alloys have no primary creep.

The differences in creep behavior between tungsten and the W-Re alloys indicate that they do not deform by the same mechanism. In addition to the differences in the shape of the creep curves, tungsten developed well defined subgrains during creep and the alloys did not, and the stress law for tungsten, where $\dot{\epsilon} \sim \sigma^{5.8}$, differed from that for the W-Re alloys, where $\dot{\epsilon} \sim \sigma^{3.8}$ (excluding the low stress—small grain size results for W-25 Re). Based on the deformation characteristics of the alloys, the likely mechanism controlling creep is either motion of jogged screw dislocations[38] or glide of dislocations.[54] For the stress range studied, the jogged screw model requires the strain-rate dependence on stress to deviate from a power law and the activation energy for creep to be dependent on the applied stress. This is contrary to the experimental data obtained for the alloys where the stress exponent is constant with temperature and the activation energy for creep is not sensitive to the applied stress. Therefore, the deformation behavior of W-Re alloys appears to be in accord with the dislocation glide mechanism.

The change in creep behavior of W-25 Re at low stresses and small grain sizes was not anticipated (Figs. 7 and 11). Under these conditions, the creep rate varies linearly with stress, and the activation energy decreases in a regular manner as stress decreases below 5000 psi to a constant value of about 62 kcal/mole. In this region, creep rate is less sensitive to temperature and stress. Obviously, a different deformation mechanism governs creep in fine-grained W-25 Re at low stresses. The direct proportionality between strain rate and stress suggests that creep could be controlled by the Nabarro-Herring mechanism[58,59] or grain boundary sliding.[60]

Examination of the microstructures of creep-tested specimens showed that W-25 Re consistently had an appreciably higher amount of grain boundary void formation when compared with the other two materials studied. Typical examples of the severe cases of void formation are shown in Fig. 26. A series of bulk density measurements as a function of strain on creep tested specimens indicated that voids formed continuously after loading. Voids on grain boundaries transverse to the applied tensile stress are more easily rationalized on the basis of the grain boundary sliding model.

The constant activation energy of 62 kcal/mole in the low stress—low grain size region apparently corresponds to the activation energy for a particular deformation mechanism, but does not correspond to any reported diffusion process. As previously discussed, the activation energy for grain boundary diffusion is around 100 kcal/mole,[43,44] so this diffusion process can be ruled out. The value of 62 kcal/mole might possibly represent the activation energy for diffusion on pore surfaces. However, a theoretical mechanism has not been proposed for creep controlled by the growth of this type of void involving surface diffusion.

CONCLUSIONS

Tungsten.

1) The apparent activation energy for creep was 100 kcal/mole and was not a function of the applied stress from 2500 to 7500 psi.

2) The secondary creep rate was dependent on stress to the 5.8 power, and the stress exponent did not vary with temperature in the region 1400-1800°C.

3) Subgrain size was inversely proportional to the applied stress and was not sensitive to temperature.

4) Dislocation density was proportional to stress to the 2.3 power and was not sensitive to temperature.

5) Primary creep was associated with subgrain formation.

6) The rate-controlling deformation mechanism during creep was ascribed to dislocation climb, and the governing diffusion process during creep was ascribed to either sub-boundary or dislocation core diffusion.

W-25 Re.

1) Two distinct rate-controlling deformation mechanisms, dependent on grain size, were operative in the temperature region 1400°-1800°C.

2) One mechanism involved an apparent activation energy for creep of 100 kcal/mole, a stress exponent of 3.8, and dislocation density proportional to stress to the 2.3 power. Creep was controlled by the dislocation glide mechanism, and was governed by dislocation core diffusion.

3) The other mechanism involved an apparent activation energy for creep of 62 kcal/mole and a stress exponent of one. Creep was attributed to grain boundary sliding. A characteristic of this mechanism was extensive void formation on grain boundaries normal to the applied stress.

4) No primary creep was evident during deformation by either mechanism under any conditions of temperature, stress, or grain size.

5) The equilibrium dislocation density during high-temperature deformation was established immediately after application of the stress.

6) Solid solution alloying of 25% rhenium with tungsten was ineffective in promoting creep resistance.

W-30 Re.

1) The apparent activation energy for creep was 100 kcal/mole and was independent of the applied stress from 2500 to 7500 psi.

2) The secondary creep rate was proportional to stress to the 3.8 power, and this relation did not change with temperature in the range 1400-1800°C.

3) Dislocation density varied as stress to the 2.3 power and was insensitive to temperature.

4) Steady-state deformation occurred without measurable primary creep, and the equilibrium dislocation density was established immediately after application of the stress.

5) The creep strength was not enhanced by σ phase precipitates in grain boundaries.

6) The rate-controlling deformation mechanism during creep was ascribed to the dislocation glide model, and the governing diffusion process during creep was ascribed to dislocation core diffusion.

ACKNOWLEDGMENTS

The authors gratefully acknowledge Gene Raymond, Andy Ruotola, and Frank Uribe for specimen preparation and mechanical testing, Sam Di Giallonardo and Harlan Olson for electron metallography, Jacquie Sipes for light metallography, and Steve Root for materials procurement. They also thank Lee Roberts for his interest and support of this investigation.

REFERENCES

[1]O. D. Sherby and P. M. Burke: Prog. Mater. Sci., 1968, vol. 13, pp. 325-90.

[2]C. R. Barrett, A. J. Ardell, and O. D. Sherby: Trans. TMS-AIME, 1964, vol. 230, pp. 200-04.

[3]C. R. Barrett and O. D. Sherby: Trans. TMS-AIME, 1965, vol. 233, pp. 1116-1119.

[4]O. D. Sherby: Acta Met., 1962, vol. 10, pp. 135-47.

[5]A. I. Blank and H. L. Burghoff: Am. Soc. Testing Mater., Proc., 1951, vol. 51, pp. 981-93.

[6]F. Garafolo, W. F. Domis, and F. Von Gemmingen: Trans. TMS-AIME, 1964, vol. 230, pp. 1460-67.

[7]C. R. Barrett, J. L. Lytton, and O. D. Sherby: Trans. TMS-AIME, 1964, vol. 239, pp. 170-80.

[8]R. R. Vandervoort: Trans. TMS-AIME, 1968, vol. 242, pp. 345-46.

[9]P. E. Armstrong and H. L. Brown: Trans. TMS-AIME, 1964, vol. 230, pp. 962-66.

[10]F. F. Schmidt and H. R. Ogden: Defense Military Information Center Report 188, Columbus, Ohio, September 1963, 240 pp.

[11]T. S. Lundy, F. R. Winslow, R. E. Pawell, and C. J. McHargue: Trans. TMS-AIME, 1965, vol. 233, pp. 1533-39.

[12]R. F. Peart, D. Graham, and D. H. Tomlin: Acta Met., 1962, vol. 10, pp. 519-23.

[13]R. Resnick and L. S. Castleman: Trans. TMS-AIME, 1960, vol. 218, pp. 307-10.

[14]J. Askill and D. H. Tomlin: Phil. Mag., 1963, vol. 8, pp. 997-1001.

[15]W. Danneberg and E. Krautz: Z. Naturforsch., 1961, vol. 16a, pp. 854-58.

[16]Y. V. Boresov, P. L. Gruzin, and L. V. Pavlinov: Metal i Metalloved, 1959, vol. 1, pp. 213-17.

[17]R. E. Pawel and T. S. Lundy: J. Phys. Chem. Solids, 1965, vol. 26, pp. 937-42.

[18]R. L. Eager and D. B. Langmuir: Phys. Rev. 1953, vol. 89, p. 911.

[19]R. L. Andelin, J. D. Knight, and M. Kahn: Trans. TMS-AIME, 1965, vol. 233, pp. 19-24.

[20]W. Danneberg: Metall., 1961, vol. 15, pp. 977-81.

[21]W. D. Klopp, W. R. Witzke, and P. L. Raffo: Trans. TMS-AIME, 1965, vol. 233, pp. 1860-66.

[22]G. W. King and H. G. Sell : Trans. TMS-AIME, 1965, vol. 233, pp. 1104-13.

[23]E. R. Gilbert, J. E. Flinn, and F. L. Yaggee: The Fourth Symposium on Refractory Metals, French Lick, Indiana, Oct. 3-5, 1965.

[24]W. V. Green: Trans. TMS-AIME, 1959, vol. 215 pp. 1057-60.

[25]High-Temperature Materials Program Progress Rep. No. 49, Part A, General Electric, Cincinnati, Ohio, July 28, 1965.

[26]J. W. Pugh: Proc. ASTM, 1957, vol. 57, pp. 906-15.

[27]H. E. McCoy: Oak Ridge National Laboratory Report No. ORNL-3992, August 1966, 50 pp.

[28]J. M. Dickinson and L. S. Richardson: Trans. ASM, 1959, vol. 51, pp. 758-771.

[29]F. Garofalo, L. Zwell, A. S. Keh, and S. Weissmann: Acta Met., 1961, vol. 9, pp. 721-29.

[30]C. R. Barrett, W. D. Nix, and O. D. Sherby: Trans-ASM, 1966, vol. 59, pp. 3-15.

[31]I. S. Servi and N. J. Grant: Trans. TMS-AIME, 1951, vol. 191, pp. 917-922.

[32]R. W. Guard: Creep and Recovery, p.251, American Society of Metals, Cleveland, Ohio, 1957.

[33]A. Goldberg: J. Iron Steel Inst., 1966, vol. 204, pp. 268-77.

[34]G. Schoeck: J. Appl. Phys., 1962, vol. 33, pp. 1745-47.

[35]R. K. Ham: Phil. Mag., 1961, vol. 6, pp. 1183-84.

[36]P. B. Hirsch et al.: Electron Microscopy of Thin Crystals, p. 422, Plenum Press, New York, 1965.

[37]B. Warlimont-Meier, P. Beardmore, and D. Hull: Acta Met., 1967, vol. 15, pp. 1399-1402.

[38]C. R. Barrett and W. D. Nix: Acta Met., 1965, vol. 13, pp. 1247-58.

[39]J. Weertman: Trans. TMS-AIME, 1960, vol. 218, pp. 364-65.

[40]J. E. Dorn: Creep and Recovery, p. 255, American Society of Metals, Cleveland, Ohio, 1957.

[41]High-Temperature Materials Program Progress Report 51A, General Electric, Cincinnati, Ohio, July 28, 1965.

[42]S. L. Robinson: DMS Report 67-30, Stanford University, Stanford, California, July 1967, 20 pp.

[43]N. C. Kothari: J. Less-Common Metals, 1963, vol. 5, pp. 140-50.

[44]T. Vasilos and J. T. Smith: J. Appl. Phys., 1964, ovol. 35, pp. 215-17.

[45]K. G. Kreider and G. Bruggeman: Trans. TMS-AIME, 1967, vol. 239, pp. 1222-26.

[46]G. M. Neumann and W. Herschwald: Z. Naturforsch., 1966, vol. 21A pp. 812-15.

[47]O. D. Sherby and J. E. Dorn, Trans. TMS-AIME, 1953, vol. 197, pp. 324-30.

[48]L. M. T. Hopkin, J. Iron Steel Inst., 1965, vol. 203, p. 583.

[49]D. McLean: Reports on Progress in Physics, 1966, Part I, vol. 29, pp. 1-33.

[50]P. B. Hirsch: The Relation between the Structure and Mechanical Properties of Metals, p. 40, Her Majesty's Stationery Office, London, 1963.

[51]E. R. Gilbert: Trans. TMS-AIME, 1966, vol. 263, p. 1511.

[52]W. D. Klopp et al.: Trans. TMS-AIME, 1966, vol. 263, p. 1511-12.

[53]J. Weertman: J. Appl. Phys. 1957, vol. 28, pp. 362-64.

[54]J. Weertman: J. Appl. Phys., 1957, vol. 28 pp. 1185-89.

[55]P. N. Flagella and C. O. Tarr: General Electric Co. Report GE-TM-65-9-12, Evandale, Ohio, April 1966, 17 pp.

[56]R. L. Stephenson: Oak Ridge National Laboratory Report ORNL-4170, June 1967, p. 89.

[57]J. C. Sawyer and E. A. Steigerwald: J. Materials, 1967, vol. 2, pp. 341-61.

[58]F. R. N. Nabarro: Report Conference Strength of Solids, (Univ. Bristol) July 1947 pp. 75-90 (published 1948).

[59]C. Herring: J. Appl. Phys., 1950, vol. 21, pp. 437-45.

[60]F. Garofalo: Fundamentals of Creep and Creep-Rupture in Metals, p. 127, MacMillan Co., New York, 1965.

Table I. Typical Specimen Impurity Content (ppm)

	W	W-25 wt.% Re	W-30 wt. % Re
Al	15	15	7
Ca	5	5	5
Cr	< 5	5	5
Cu	15	10	< 1
Fe	35	12	15
Mg	3	2	< 1
Ni	< 5	7	5
Si	< 10	< 10	10
H	< 1	< 1	< 1
C	6	10	65
N	2	1	2
O	8	10	10

Table II. Electropolishing Conditions to Prepare Foils for Examination by Transmission Electron Microscopy

Material	Electrolyte	Temperature (°C)	Voltage
W	2% NaOH	0	15
W-25 wt. % Re W-30 wt. % Re	92.5 ml methyl alcohol +5.0 ml H_2SO_4 +2.5 ml HF	-40	25

FIGURE CAPTIONS

Fig. 1. Effect of temperature on the elastic modulus of refractory metals.

Fig. 2. Diffusion coefficients for refractory metals.

Fig. 3. Tungsten-rhenium system.[28]

Fig. 4. Creep curves for tungsten, W-25 wt. % Re, and W-30 wt. % Re at 1700°C and 5000 psi.

Fig. 5. Schematic of the shape of the creep curves during change of temperature tests for tungsten, W-25 wt. % Re, and W-30 wt. % Re.

Fig. 6. The effect of stress on strain rate for tungsten.

Fig. 7. The effect of stress on strain rate for W-25 wt. % Re.

Fig. 8. The effect of stress on strain rate for W-30 wt. % Re.

Fig. 9. Schematic of the shape of the creep curves during change of temperature tests for tungsten, W-25 wt. % Re, and W-30 wt. % Re.

Fig. 10. Activation energy for creep of tungsten.

Fig. 11. Activation energy for creep of W-25 wt. % Re.

Fig. 12. Activation energy for the creep of W-30 wt. % Re.

Fig. 13. The effect of grain size on strain rate for W-25 wt. % Re.

Fig. 14. Dislocation networks in tungsten creep tested to a strain of 5% at 10,000 psi and 1700°C.

Fig. 15. Dislocation substructure in W-25 wt. % Re creep tested to a strain of 5% at 10,000 psi and 1700°C.

Fig. 16. Dislocation substructure in W-30 wt. % Re creep tested to a strain of 5% at 10,000 psi and 1700°C.

Fig. 17. The relationship between subgrain size and stress for tungsten creep tested to a strain of 5% at 1700°C.

Fig. 18. Examples of subgrains in tungsten creep tested to a strain of 5% at 10,000 psi and 1700°C.

Fig. 19. The influence of stress on dislocation density for tungsten, W-25 wt. % Re, and W-30 wt. % Re creep tested to a strain of 5% at 1700° C.

Fig. 20. The change in dislocation density as a function of stress for W-25 wt. % Re creep tested to a strain of 5% at 1700° C.

Fig. 21. Comparison of drop-in-stress creep test and standard creep test for tungsten.

Fig. 22. Comparison of creep data for polycrystalline tungsten at temperatures between 0.5 and 0.67 T_m. Data normalized by $Z = \dot{\epsilon} e^{\Delta H/RT}$ (ΔH = 100 kcal/mole).

Fig. 23. Comparison of creep data for polycrystalline W-25 wt. % Re alloy at temperatures between 0.5 and 0. 67 T_m. Data normalized by $Z = \dot{\epsilon} e^{\Delta H/RT}$ (ΔH = 100 kcal/mole).

Fig. 24. Interaction between dislocations and σ phase particles in W-30 wt. % Re alloy creep tested at 1700°C.

Fig. 25. Comparison of creep data for tungsten and W-Re alloys.

Fig. 26. Grain boundary voids in specimens creep tested to a strain of 5% at 3500 psi and 1700°C.

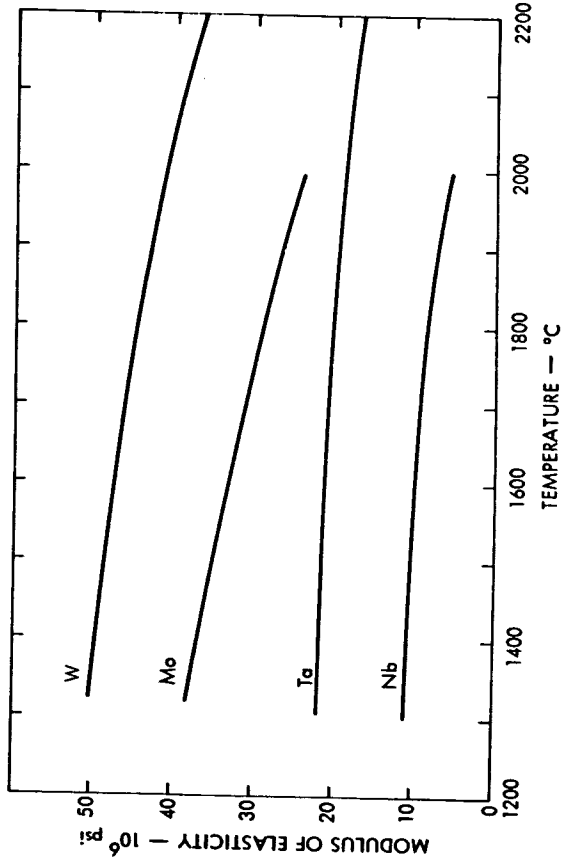

Vandervoort - Fig. 1

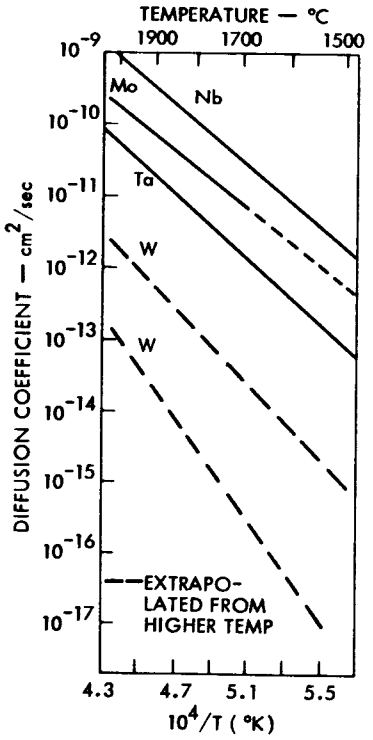

Vandervoort - Fig. 2

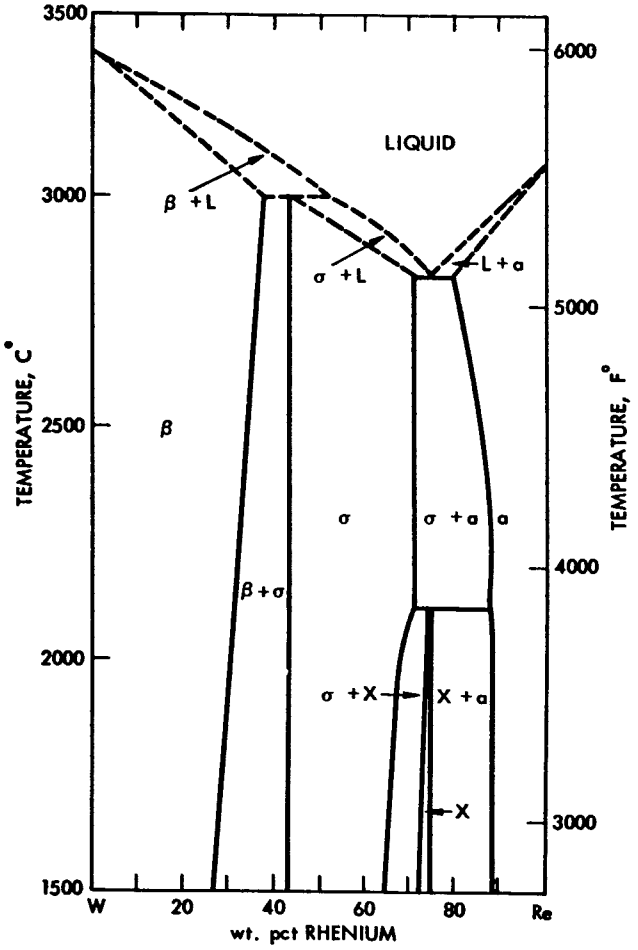

Vandervoort - Fig. 3

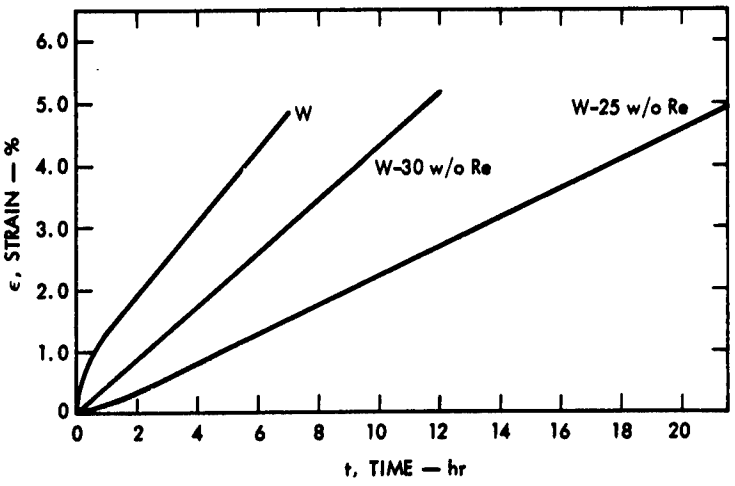

Vandervoort - Fig. 4

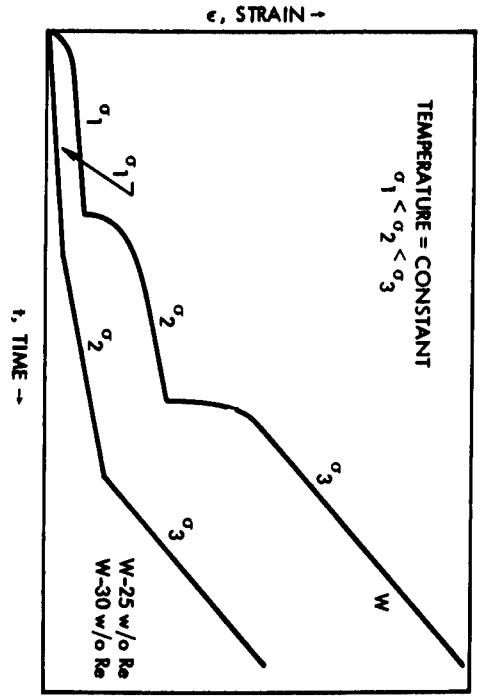

Vandervoort - Fig. 5

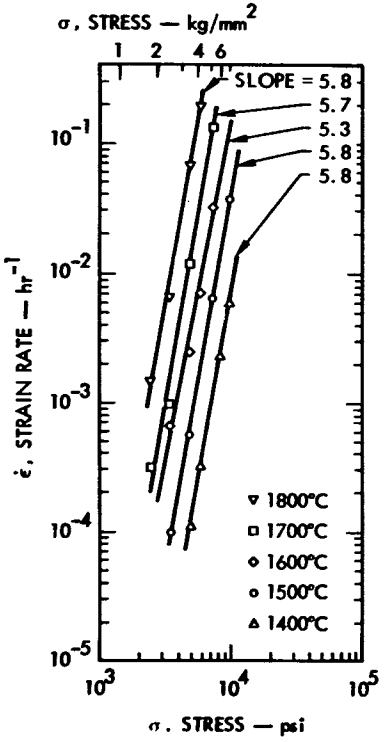

Vandervoort - Fig. 6

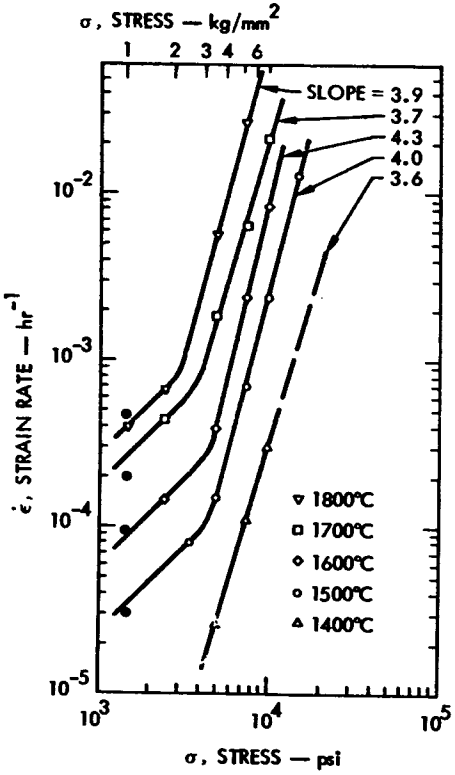

Vandervoort - Fig. 7

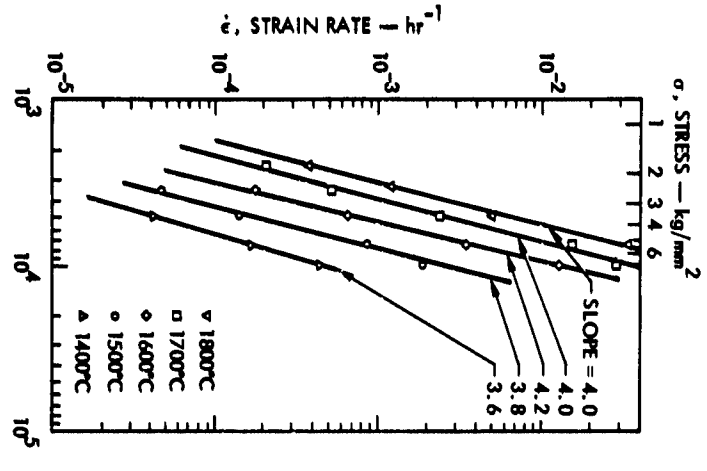

Vandervoort - Fig. 8

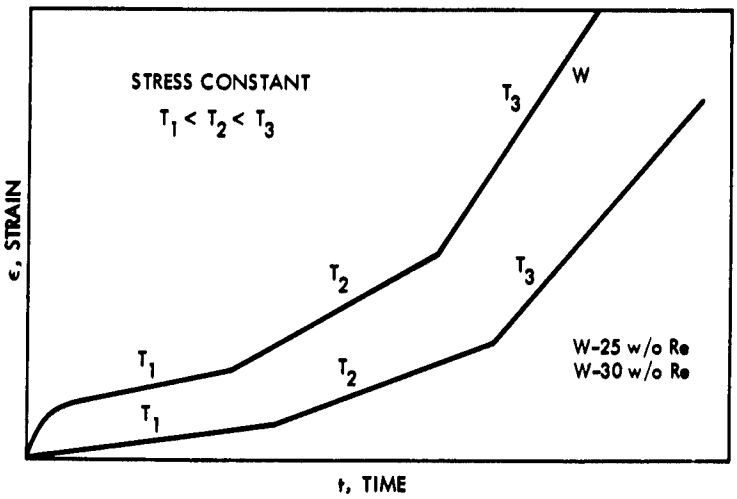

Vandervoort - Fig. 9

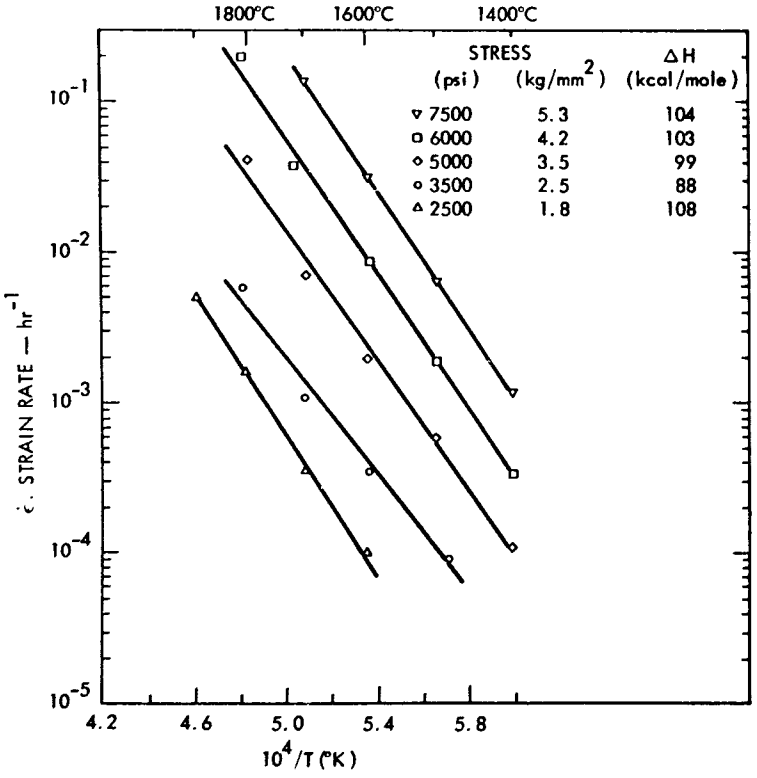

Vandervoort - Fig. 10

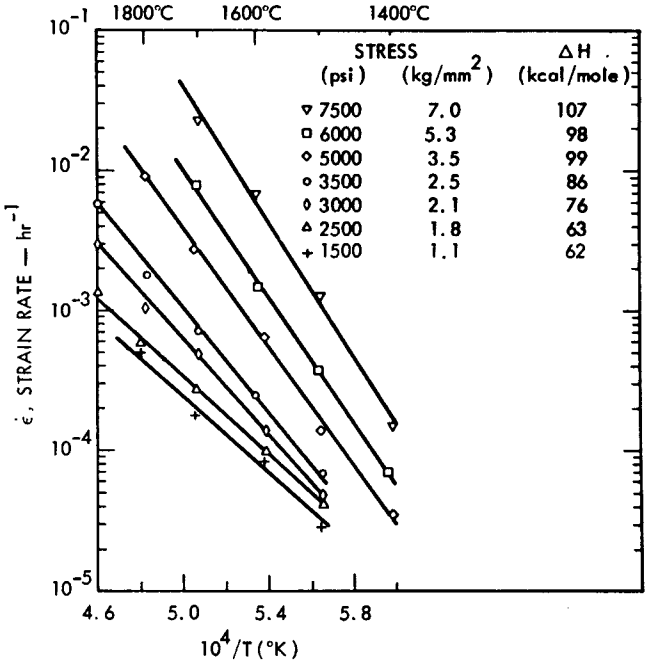

Vandervoort - Fig. 11

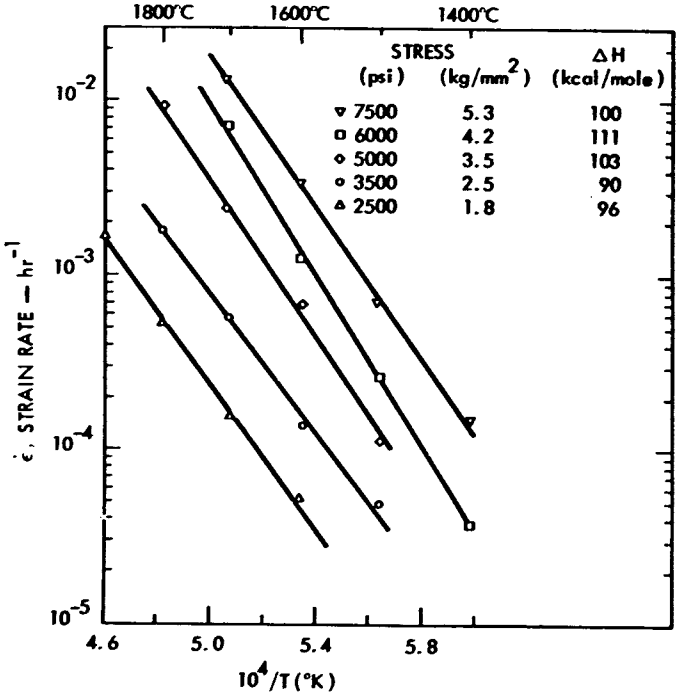

Vandervoort - Fig. 12

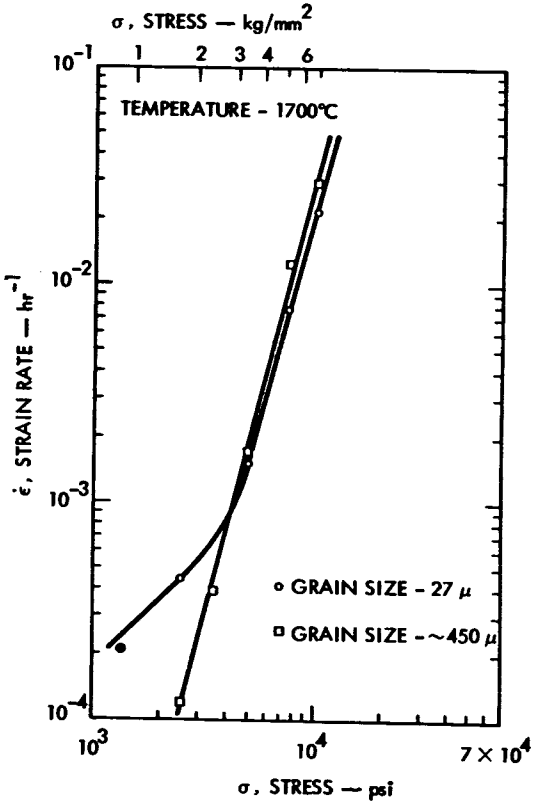

Vandervoort - Fig. 13

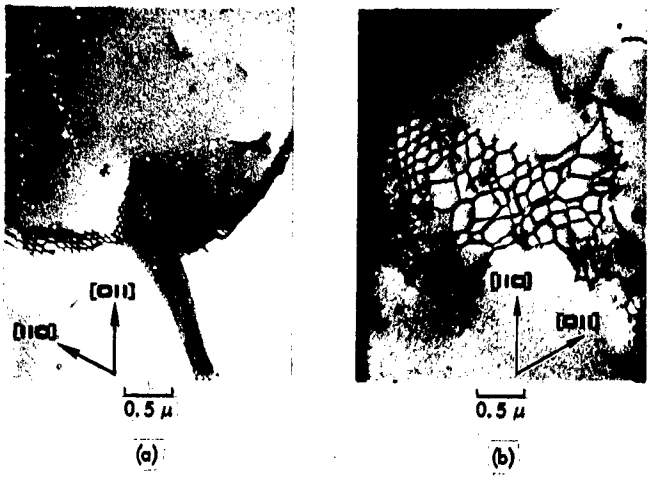

Vandervoort - Fig. 14

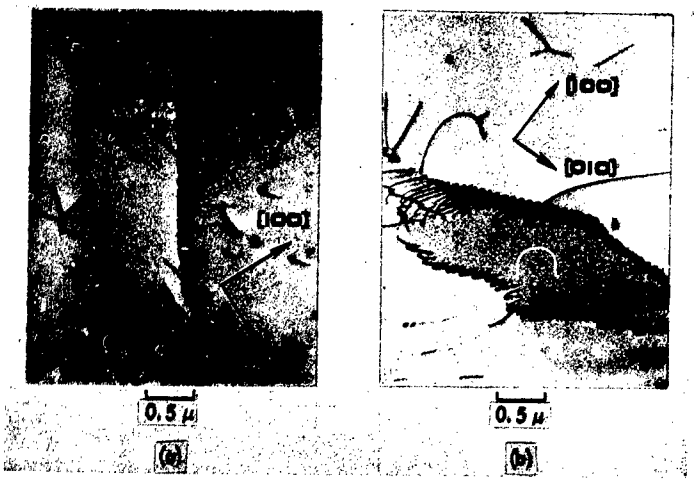

Vandervoort - Fig. 17

Vandervoort - Fig. 18

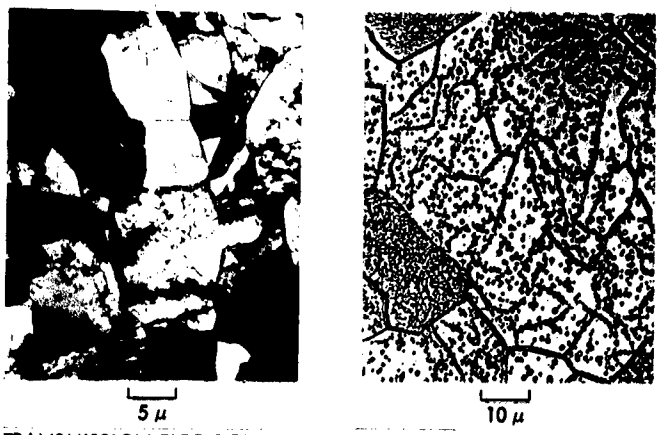

TRANSMISSION ELECTRON MICROSCOPY

ETCH PITS

Vandervoort - Fig. 18

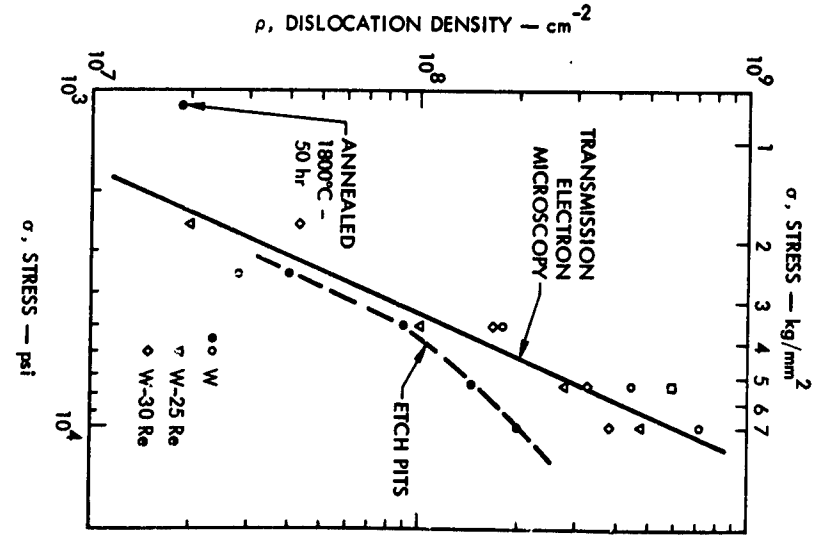

Vandervoort - Fig. 19

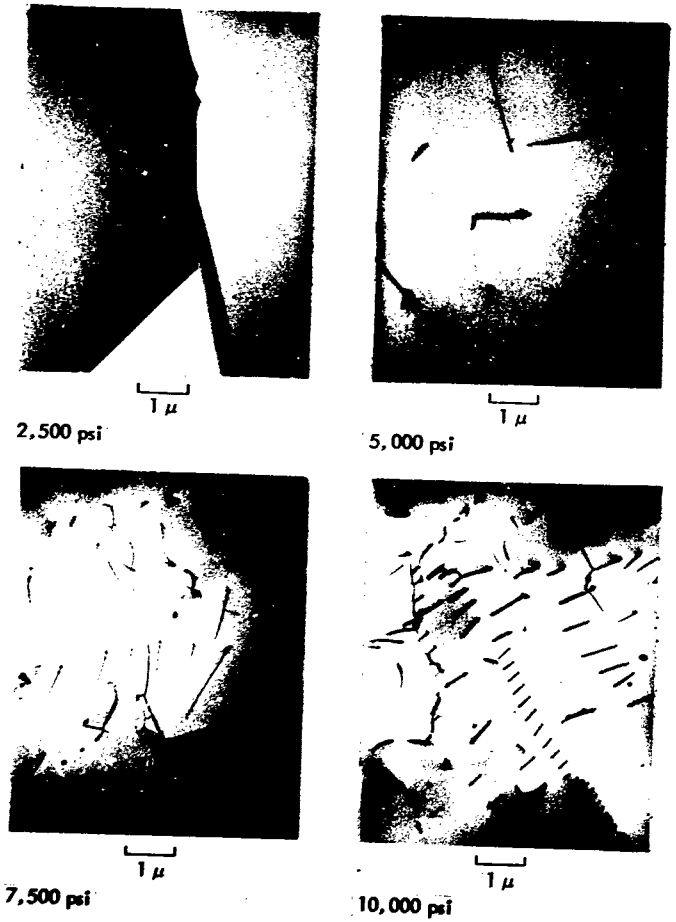

Vandervoort - Fig. 20

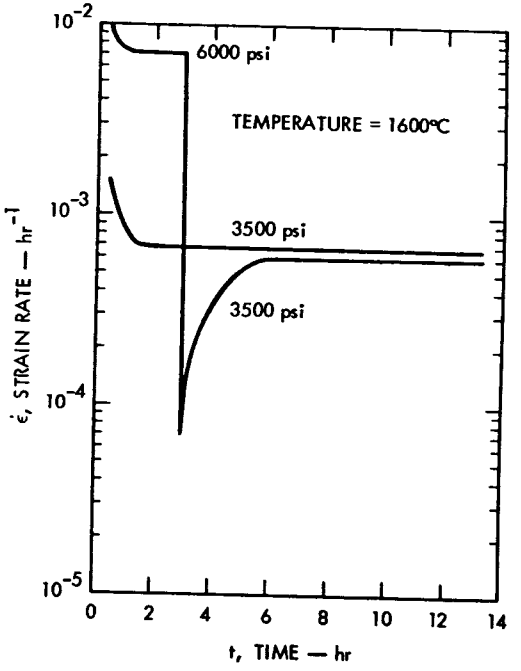

Vandervoort - Fig. 21

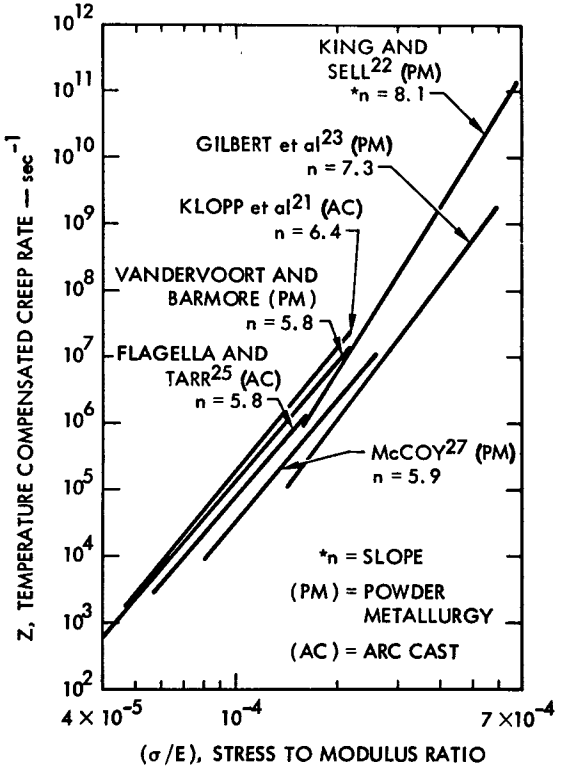

Vandervoort - Fig. 22

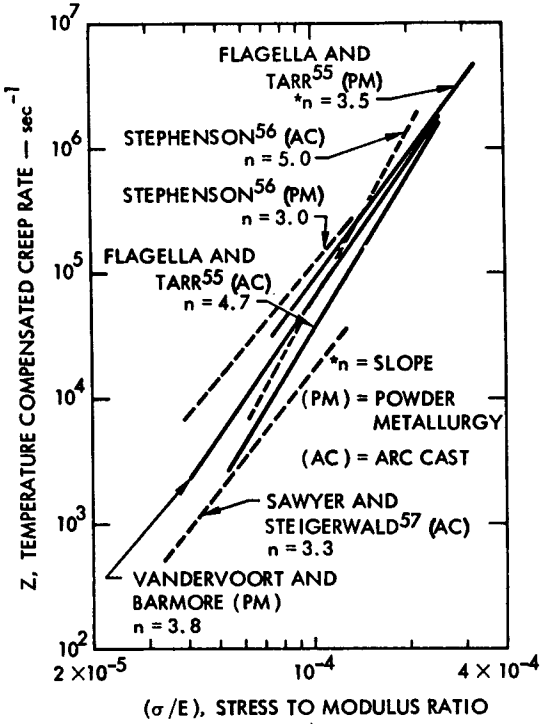

Vandervoort - Fig. 23

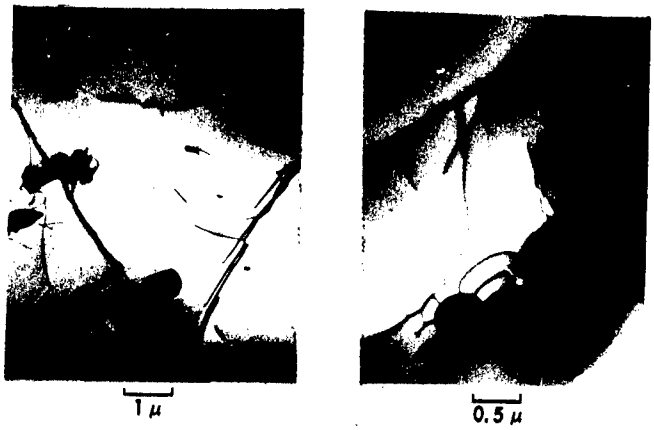

Vandervoort - Fig. 24

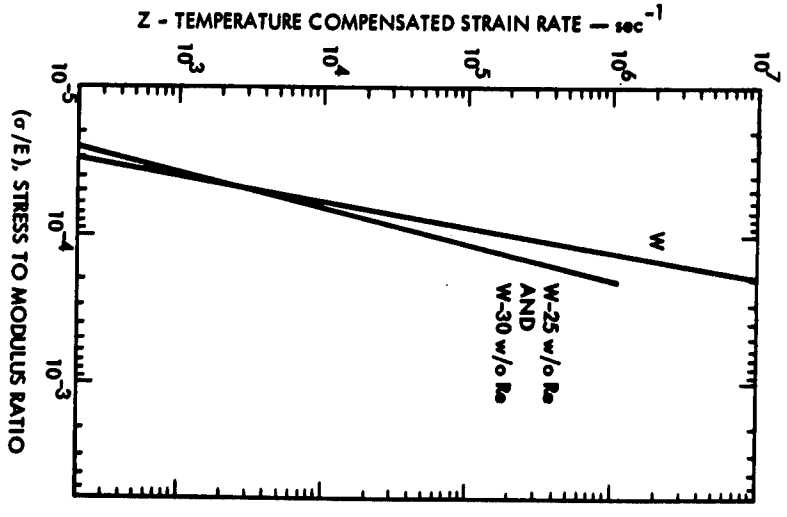

Vandervoort - Fig. 25

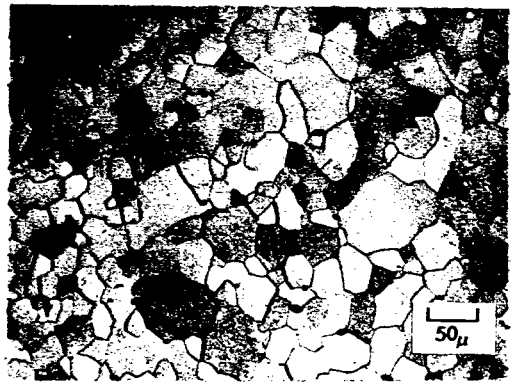

TUNGSTEN

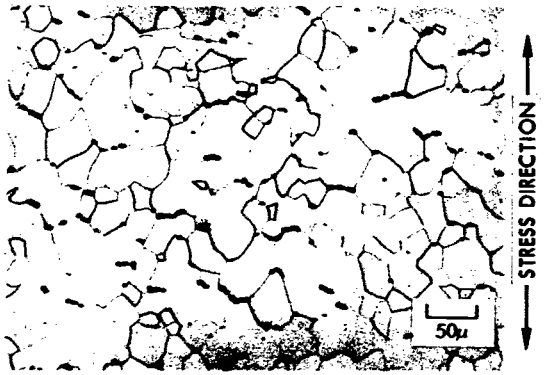

TUNGSTEN-25 w/o RHENIUM

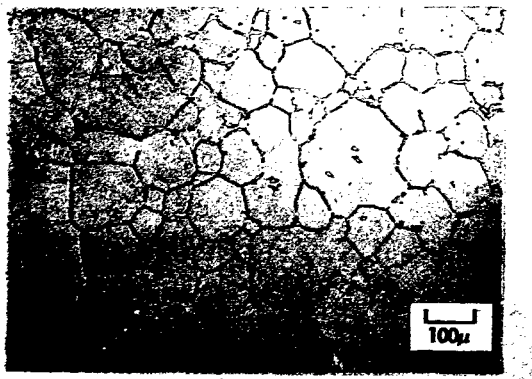

TUNGSTEN-30 w/o RHENIUM | Vanderwoort - Fig. 2E

1. Fauv ✓
2. McCall

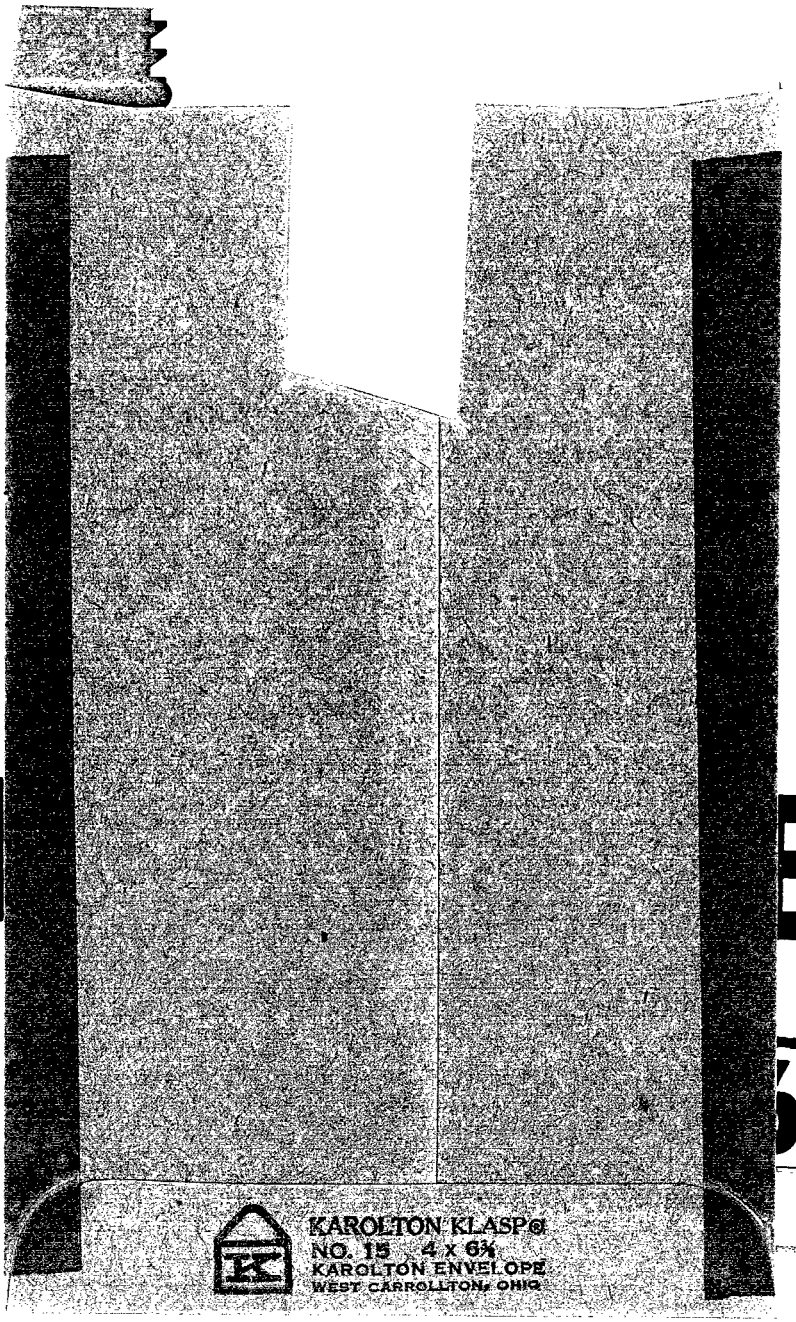

ED

9